MECH.4991: Directed Study

Technical Report: Aircraft Design - Aerodynamics

Hoang Pham

05/06/2022

I. Introduction

To ensure an aircraft can fly safely while maintaining its functional purpose (transportation, cargo handling, etc.) has always been a challenging problem for engineers. As a result, the design of aircraft must be conducted in a systematic way, and it is usually broken down into three stages: conceptual design, preliminary design, and detail design. The conceptual and preliminary design stages are critical since the layout for the aircraft will be selected, and the initial sizing of components will also be chosen. These two steps provide a guideline for future steps and iterations in the design process. Thus, different methodologies will be explored to perform the conceptual and preliminary stages, with a focus on aerodynamics, for the design of an aircraft for the AIAA Design Build Fly competition. The goal of this project was to gain a better understanding of the design process while laying out a foundation to fabricate a competitive aircraft for DBF.

II. Methodology

1. Conceptual Design

Conceptual design is the first and most important step in the design process for an aircraft. This step involves selecting a path forward for the design and the development of a preferred system, which is highly dependent on the requirement for the project and the limitation of resources [1]. For this stage, general requirements for the aircraft will be evaluated to generate satisfactory configurations for the aircraft. The conceptual design stage requires evaluations and analyses, and only a few calculations are conducted. The output of this design phase is a general layout for the aircraft, which entails the wing, fuselage, tail, engine, and landing gear. However, with a focus on aerodynamics, the wing and tail configurations were analyzed and selected.

1.1 Wing Configuration

For an aircraft competing in the DBF competition, two components for the wing were determined from an early stage: wing location and wing planform.

Firstly, the wing location influences the design of other components such as the tail design, landing gear design, and the aircraft's center of gravity. There are three general wing configurations: low wing, mid wing, and high wing. Each type has its own advantages and disadvantages. As a result, a trade study using a decision matrix was conducted in order to select the most appropriate wing location. Different criteria such as stability, structural strength, manufacturability, and cargo space were ranked based on importance by assigning a weight (1-5). The three wing configurations were then scored from 1 to 10 for each category, and the total weighted sums of the scores were compared in order to select the best wing location.

Secondly, the planform has a significant influence on the aerodynamics performance of the wing. It dictates the lift distribution and the induced drag of the wing, which directly affects the range and efficiency of the aircraft. For larger aircraft, this is usually decided at a later stage with further calculations since it is of high importance. However, for an aircraft competing in the DBF competition, this criterion must be analyzed early on since (unlike professional aircraft) the manufacturing processes are limited for smaller RC aircraft. As a result, for the conceptual design stage, a trade-off study for the wing planform was also conducted similar to the wing location study.

1.2 Tail Configuration

Similar to the wing configuration, the tail configuration must also be selected early through reasoning, logic, and evaluation. The optimal tail configuration was chosen using four requirements: stability and control, structural strength, manufacturability, and efficiency. Aircraft tail configurations have been studied and analyzed thoroughly, and there are a few main types: conventional, T-tail, cruciform, H-tail, V-tail, twin vertical tail, and boom-mounted [1]. However, for a small DBF aircraft, with the limitations of manufacturing for both the tail and the fuselage shape, only the conventional tail, T-tail, and H-tail were analyzed during the conceptual design stage. These three configurations were evaluated using another decision matrix.

2. Preliminary Design

In contrast to the conceptual design stage, the preliminary design outcomes are a result of calculation procedures. However, the parameters determined for this stage are not final and usually require iterations through feedback from high fidelity simulations, experiments, or even test flights. The calculated dimensions provide a good starting point for design, and they significantly affect the detail design phase.

2.1 MTOW estimation

The maximum takeoff weight estimation was conducted based on historical data. For this step, data from past aircraft was used in order to approximate the MTOW of the aircraft. This estimation has around 20% inaccuracies; thus, the estimation must be changed when the components of the aircraft have a more concrete design.

In order to determine the MTOW, the ratio of the empty weight W_E to the maximum takeoff weight W_{TO} for several top-performing aircraft from the DBF competition was determined from previous reports. Since most of the components for this year's aircraft (battery, servo, motor, etc.) were similar to the last year's, the empty weight was readily calculated. With the ratio W_E/W_{TO} and the W_E known, the maximum takeoff weight was estimated.

2.2 Wing area sizing

With the MTOW estimated, the required area of the wing was determined using Sadraey's method [1]. The weight to power ratio was calculated as a function of the wing loading and different parameters: stall velocity, maximum velocity, maximum takeoff length, rate of climb, and maximum altitude.

The wing loading can be represented as a function of the stall speed as:

$$\left(\frac{W}{S}\right)\Big|_{V_S} = \frac{1}{2}\rho V_s^2 C_{L_{max}} \tag{1}$$

where W is the weight, S is the wing area, V_S is the stall speed, ρ is the density, and $C_{L_{max}}$ is the maximum aircraft lift coefficient.

This provided an upper limit for the wing loading with a specified V_S. The air density must be chosen at sea level since it provides the lowest stall speed. The maximum lift coefficient is not determined at this point; as a result, Sadraey's recommended a value of 1.5 [1] for these types of aircraft.

For the maximum velocity, the weight to power ratio can be represented as a function of the wing loading as:

$$\left(\frac{W}{P}\right) = \frac{\eta_P}{\frac{1}{2}\rho V_{max}^3 C_{D_o} \frac{1}{\left(\frac{W}{S}\right)} + \frac{2K}{\rho V_{max}}\left(\frac{W}{S}\right)} \tag{2}$$

where P is the power, V_{max} is the max speed, η_P is the propeller efficiency, C_{D_o} is the zero-lift drag coefficient, and K is the induced drag factor.

The V_{max} was specified to be 98.4 ft/s, and the value was attainable according to propulsion simulations. η_p was chosen to be 0.75, C_{D_o} was chosen to be 0.0325, and K was chosen to be 0.0680. These values are difficult to determine at this stage. As a result, all the values are based on previous aircraft data suggested by Sadraey [1].

Similar equations were derived and suggested by Sadraey. After the equations were calculated, the functions were plotted using MATLAB (Appendix A) to determine a design region for the aircraft, and a design point was chosen as a starting point for the wing loading.

2.3 Airfoil selection

After the wing loading had been determined, the airfoil for the wing was selected. The cruise lift coefficient can be calculated as:

$$C_{L_C} = \frac{2W}{\rho V_C^2 S} = \frac{2}{\rho V_C^2}\left(\frac{W}{S}\right) \tag{3}$$

where V_c is the cruise speed.

Generally, Sadraey [1] suggests that $V_{max} = 1.2V_c$; therefore, the cruise velocity for the aircraft was 82 ft/s based on the target max speed. Therefore, the cruise lift coefficient for the aircraft can be estimated. Since lift is also generated by different components other than the wing, the wing lift coefficient was estimated [1] as:

$$C_{L_{C_w}} = \frac{C_{L_C}}{0.95} \tag{4}$$

The ratio between the wing cruise lift coefficient and the aircraft cruise lift coefficient is highly dependent on the configuration of the aircraft. However, during the preliminary phase, a concrete relationship cannot be determined. As a result, the above estimation was used as a starting point for the design. The relationship can be recalculated during future design phases through complex simulation or wind tunnel testing.

From the wing cruise lift coefficient, the ideal airfoil lift coefficient was estimated using Sadraey's recommendation [1]:

$$C_{l_i} = \frac{C_{L_{C_w}}}{0.9} \tag{5}$$

Again, this relationship was used for the preliminary design phase since the geometry for the wing has not yet been determined.

The same calculations were used to determine the maximum lift coefficient for the airfoil.

$$C_{L_{max}} = \frac{2}{\rho V_s^2}\left(\frac{W}{S}\right) \tag{6}$$

$$C_{L_{max_w}} = \frac{C_{L_{max}}}{0.95} \tag{7}$$

$$C_{l_{max}} = \frac{C_{L_{max_w}}}{0.9} \tag{8}$$

However, the max airfoil lift coefficient can also include the effects of high-lift devices. Therefore, more options were available since the maximum lift coefficient of the airfoil could still be lower than the calculated value, given that the HLD can provide the required lift increment.

With the maximum lift coefficient determined, several airfoils were selected and evaluated to select the optimum.

2.4 Wing sizing

With the wing area and the airfoil selected, the initial geometry for the wing was determined. The lift to drag ratio for several wing AR was analyzed using XFLR5, and a trade study was conducted in order to select the appropriate dimensions for the wing. Additionally, the lift distribution was also compared to the ideal elliptical lift distribution to confirm the selected parameters. With the dimensions of the wings calculated, the setting angle was determined based on the $C_{L_{C_W}}$ calculated prior.

2.5 Tail sizing

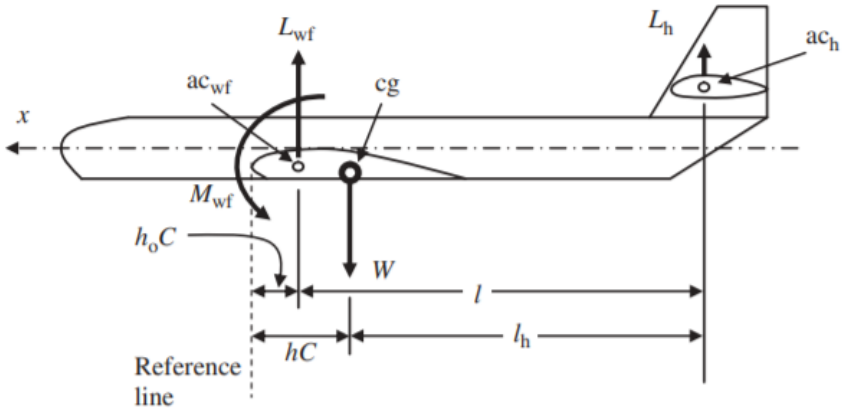

Figure 1: Horizontal tail design [1]

The horizontal tail was designed using the simplified non-dimensional longitudinal trim equation at cruise [1]:

$$C_{m_{o_{wf}}} + C_L(h - h_0) - \eta_H \bar{V}_H C_{L_H} = 0 \tag{9}$$

where $C_{m_{o_{wf}}}$ is the aircraft pitching moment coefficient, h is the normalized distance from the leading edge of the wing to the C.G, h_0 is the normalized distance from the leading edge of the wing to the aerodynamic center of the wing.

The tail volume coefficient is defined as:

$$\bar{V}_H = \frac{l}{c}\frac{S_H}{S} \tag{10}$$

Due to the effects of downwash and sidewash, the airflow through the horizontal wing tends to have a lower dynamic pressure compared to the aircraft dynamic pressure. As a result, the ratio between the dynamic pressure at the tail and the aircraft dynamic pressure can be defined as the tail efficiency:

$$\eta_H = \left(\frac{V_H}{V}\right)^2 \tag{11}$$

According to Sadraey [1], this value typically falls between 0.85 and 0.95. As a result, η_H was assumed to be 0.9 for the initial design point for the tail.

Since the initial dimensions of the wing were approximated, the pitching moment can be determined. The geometry for the aircraft had not been fully determined at the preliminary design stage; therefore, h and h_0 had to be approximated as 0.2 and 0.25 [1].

The tail volume coefficient has a significant effect on the stability of the aircraft. A higher value for the tail coefficient corresponded to a more stable (but less maneuverable) aircraft. However, for the DBF competition, a cargo aircraft was assumed. As a result, a tail coefficient of 0.5 was selected based on Sadraey's [1] recommendation for a fairly stable aircraft. The vertical tail was designed using a method.

2.6 Control surface sizing

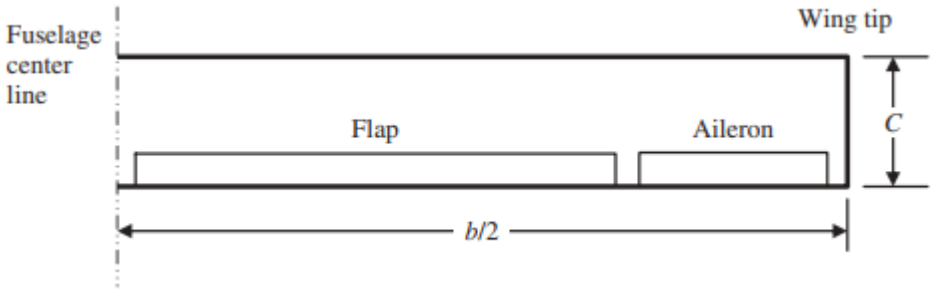

Figure 2: Flaps and ailerons on the wing [1]

The control surfaces were designed using a MATLAB script [1] (Appendix A) using the lifting line theory. The lift of the wing was calculated based on the span, chord, and flap angle during takeoff. The three parameters were iterated until the required lift during takeoff was achieved. Afterward, for ease of manufacture, the aileron was assumed to take up the remaining span of the wing.

Sadraey [1] suggested that the change in zero-angle of attack of an airfoil with flap can be estimated:

$$\Delta\alpha_0 \approx -1.15\frac{c_f}{c}\delta_f \tag{12}$$

where c_f is the flap chord, c is the wing chord, and δ_f is the flap angle.

This relationship was tested through the XFoil simulation.

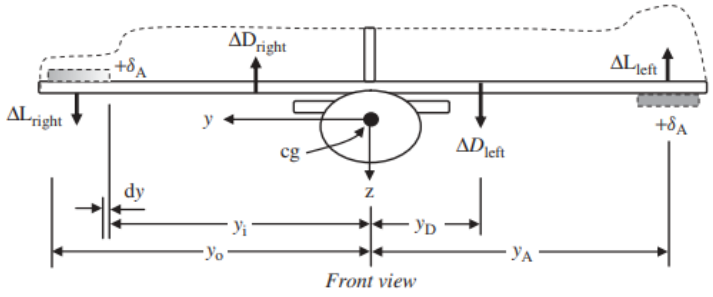

Figure 3: Ailerons analysis [1]

In future design steps, the dimensions for the aileron can be verified based on the required roll rate of the aircraft. From Figure 3, the total aerodynamic rolling moment can be shown as:

$$\sum M_{cg_x} = 2\Delta L \cdot y_A - \Delta D \cdot y_D \tag{13}$$

However, the roll analysis requires the moment of inertia of the plane about the x-axis. Therefore, this analysis cannot be conducted during the preliminary design phase, and it can only be determined when more components of the aircraft have been designed.

2.7 Takeoff distance

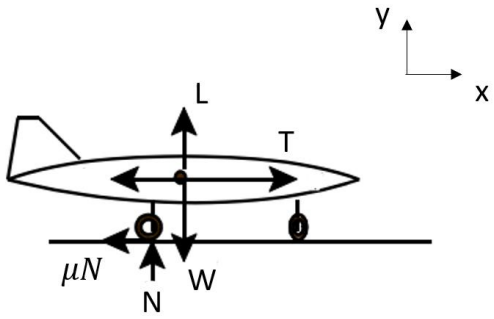

Figure 4: Forces during takeoff

For the DBF competition, a maximum takeoff distance of 25 ft was required. As a result, a quick validation was utilized to calculate the takeoff distance of the aircraft.

From the free body diagram in Figure 4, in the x-direction:

$$T - D - \mu N = m\frac{dV}{dt} \tag{14}$$

where T is the thrust, D is the drag, N is the normal force, μ is the friction coefficient, m is the mass, and t is time.

In the y-direction:

$$W - L = N \tag{15}$$

Additionally, since the aircraft is assumed to be at constant power during takeoff, the thrust can be assumed as:

$$T = \frac{P}{V} \tag{16}$$

Equations 15 and 16 can be substituted in Equation 14, and the lift and drag terms can be expressed as a function of the velocity. Additionally, the time derivative of the velocity can also be discretized using forward time difference. Therefore, the discretized form of Equation 14 can be expressed as:

$$V^{k+1} = V^k + \frac{\Delta t}{m}\left[\frac{P}{V^k} - \frac{1}{2}\rho(V^k)^2 C_D S - \mu\left(W - \frac{1}{2}\rho(V^K)^2 C_L S\right)\right] \tag{17}$$

where k represents the time step.

The lift and drag coefficients are constants based on the flap configuration of the aircraft during takeoff. As a result, the velocity and the lift can be calculated at discrete time steps. When the left exceeds the weight, the aircraft is assumed to have taken off. The total takeoff distance can be calculated by numerically integrating the velocity. The takeoff distance was analyzed using this method through a MATLAB script (Appendix A) to ensure the takeoff distance was within 25 ft.

III. Results and Discussion

1. Conceptual design

1.1 Wing Configuration

Table 1: Decision matrix for the wing configuration

Wing Configuration		**Low Wing**	**Mid Wing**	**High Wing**
Categories	Weight [1-5]	Value [1-10]	Value [1-10]	Value [1-10]
Stability	5	5	6	8
Structural Strength	4	8	6	9
Manufacturability	4	7	6	7
Cargo Space	3	7	5	8
Total		106	93	**128**

Table 1 shows the decision matrix utilized to select the wing location. From the table, it can be seen that the high wing was the optimal configuration for the aircraft. The high wing configuration allows for a single beam to be used as a support for the entire wing (instead of two cantilevers), which allows for high structural strength. The high wing configuration also has an increased dihedral effect, which allows the aircraft to be more laterally stable. Additionally, the wing only requires one mounting point on top; therefore, the manufacturing process will be quicker, and there will be more space for the cargo. For future competitions, the weight for these criteria can be changed, and scoring can also be modified depending on the specific mission requirements. Furthermore, more criteria. such as ground clearance or takeoff distance, to achieve a more detailed selection.

1.2 Wing Planform

Table 2: Decision matrix for the wing planform

Wing Planform		**Rectangular**	**Tapered**	**Elliptical**
Categories	Weight [1-5]	Value [1-10]	Value [1-10]	Value [1-10]
Aerodynamics	3	6	8	10
Controllability	4	8	7	6
Structural Strength	4	7	8	4
Manufacturability	5	9	7	6
Total		**123**	119	100

Table 2 shows the selection for the wing planform. From the table, the rectangular planform was the best option for this year's competition due to its manufacturability, and the control surfaces can be easily implemented, which highly affects the controllability. The aerodynamic and structural strength of the rectangular planform is not as good as the other options; however, this can be improved by sizing the wing correctly. Similar to the previous decision matrix, more options such as twisted wings or sweep wings may also be considered; however, these configurations are usually difficult to implement due to limitation on the manufacturing of RC aircraft.

1.3 Tail configuration

Table 3: Decision matrix for the tail configuration

Tail Configuration		**Conventional**	**T-Tail**	**H-Tail**
Categories	Weight [1-5]	Value [1-10]	Value [1-10]	Value [1-10]
Stability & Control	5	9	8	6
Structural Strength	5	7	6	5
Manufacturability	3	8	7	5
Efficiency	2	5	8	9
Total		**114**	107	88

Table 3 shows the decision matrix for the tail configurations. For this year, the optimal configuration is the conventional tail. This type of configuration allowed the plane to be easier to control since it requires only one rudder and one elevator, compared to two rudders for the H-tail. The conventional tail can be mounted directly on the fuselage, which can provide more structural strength compared to the other two configurations. Additionally, conventional tails are also easy to manufacture. The only disadvantage of this configuration is that the tail may be affected by the wing wake; however, if the aircraft was designed to not exceed a certain angle of attack, this can be prevented. For future competitions, more tail configurations can also be compared to each other. The list of tail configurations is mentioned in the design methodology section.

2. Preliminary design

2.1 MTOW estimation

Table 4: Weight ratio for top performing aircraft

Team	W_E/W_{TO}
Georgia Tech (2012) [2]	0.25
UCI (2012) [2]	0.35
Georgia Tech (2008) [3]	0.32
VTJI (2017) [4]	0.31
Georgia Tech (2016) [5]	0.25
Average	0.30

Table 4 shows the ratio of the empty weight to the max takeoff weight of the aircraft for several top performing teams in previous DBF competitions. From there, the average of these ratios can be used to option an estimation for the max takeoff weight of this year's aircraft.

Since the empty weight of the aircraft was estimated as 2.15 lb (Appendix B). Therefore, the initial assumption for the max takeoff weight of the aircraft was:

$$W_{TO} = 7.24\ lb$$

This number can be further revised when more components of the aircraft are designed. From there, the sizing of the wing can be changed accordingly. This requires multiple iterations for the design process.

For future years, more data can be utilized to refine the weight ratio.

2.2 Wing area sizing

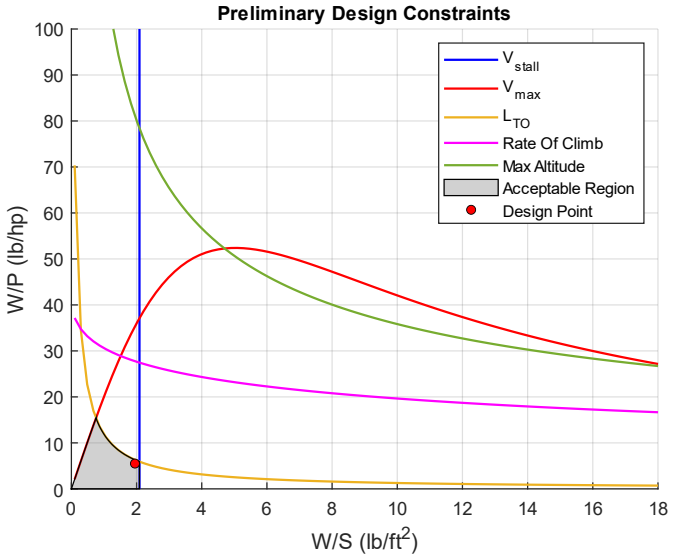

Figure 5: Acceptable design region for the aircraft

After the maximum takeoff weight was estimated, the wing loading was chosen in order to conduct the wing sizing. Figure 5 shows the weight-to-power ratio as a function of the wing loading along

with several other parameters. For each line, the region on the left (or below for the V_{max} and rate of climb line) represents design points which satisfy the chosen requirements. The regions intersect and generate an envelope which significantly restricts the design area, making it easier to pick an initial design point of 2 lb/ft^2 for the wing loading. Figure 5 was created based on the criteria for this year's competition, and the velocity was confirmed by propulsion to be obtainable. As a result, for future years, the MATLAB program (Appendix A) can be modified to achieve the design region for that year's specific requirements, and it is recommended to read more information about this method in ref [1].

From there, for this year, based on the estimated weight and wing loading, the wing area was estimated as:

$$S = 3.62\ ft^2$$

2.3 Airfoil selection

With the wing loading determined, the required lift coefficient for the airfoil was calculated using Equations 3 to 6 as:

$$C_{l_i} = 0.306$$

$$C_{l_{max}} = 1.33$$

From there, different airfoils that can achieve these requirements were identified using online resources, and their properties were compared through the XFoil simulation results.

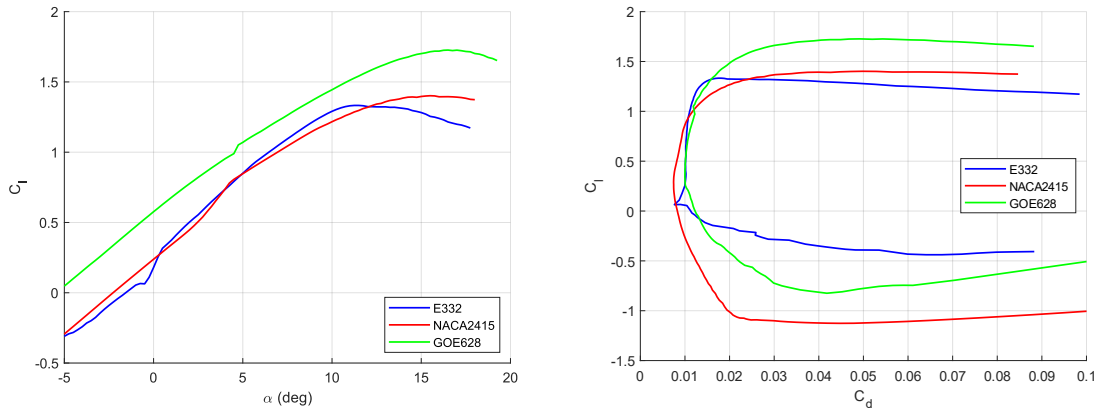

Figure 6: Comparison between different airfoils

Table 5: Summary of airfoil parameters

$Airfoil$	$C_{l,max}$	$C_{d,min}$	$Stall\ Angle\ (deg)$
E332	1.33	0.0076	11.3
NACA 2415	1.40	0.0075	15.5
GOE 628	1.73	0.0100	16.5

The airfoils simulated were E332, NACA 2415, and GOE 628 (Figure 6). The lift curves of the three airfoils along with the drag polar were evaluated to select the best option. NACA 2415 was chosen as the optimal airfoil for this year's aircraft since it met the requirements shown above, and it also had an acceptable drag coefficient and stall angle. The E332 airfoil had similar characteristics; however,

it had a much lower stall angle, which can be difficult to design around. The GOE 628 airfoil produced significantly more drag compared to the NACA 2415 airfoil, and it is also thicker, which adds more weight to the aircraft. For future years, this method can be used in a similar manner by searching for multiple airfoils which meet the lift coefficient requirements, and a trade study between the selected ones can be conducted.

In general, symmetrical airfoils are usually picked for the tails since during flight both position and negative lift coefficient are required for longitudinal stability. The vertical tail airfoil must be symmetrical due to the yaw stability requirement. As a result, the NACA 0009 airfoil was selected. For future years, a trade study can also be conducted for multiple symmetrical airfoils to select the optimum.

2.4 Wing sizing

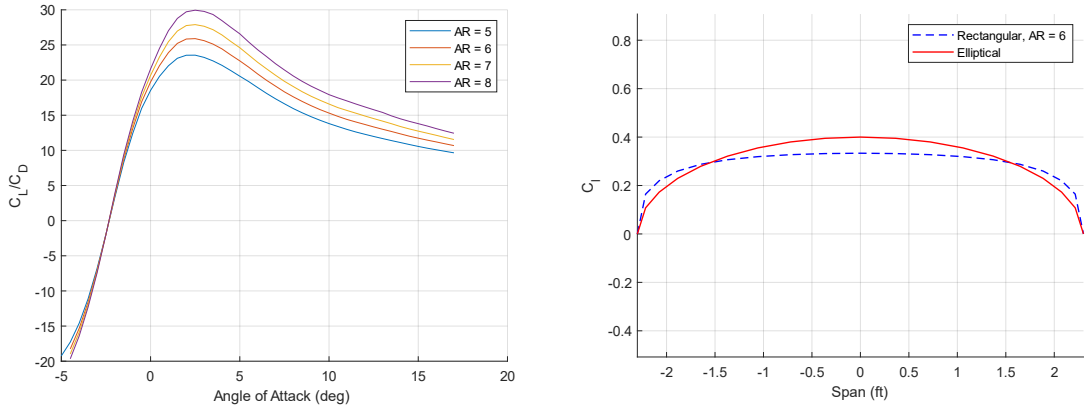

Figure 7:C_L/C_D vs angle of attack for different AR (left) and wing lift distribution (right)

In order to calculate the dimensions of the wing, the aspect ratio was decided through a trade study. Different AR simulations were conducted using XFLR5 and the C_L/C_D was plotted against the angle of attack. As seen in Figure 7, higher aspect ratios provide a high C_L/C_D. However, wings with high AR would require more support for structural strength, and the roll maneuver would also decrease. Low aspect ratios are the exact contrary. As a result, an AR of 6 was chosen, as it provided an acceptable C_L/C_D without having to sacrifice structural strength. The lift distribution was also compared to the ideal elliptical lift distribution to confirm the wing's aerodynamics capabilities. For future years, different ARs can be used. For example, if a more maneuverable aircraft is desired based on the DBF's mission requirement, an AR of 5 can be chosen. Additionally, if better materials or manufacturing processes are available, high AR could also be utilized.

With the AR known, the dimensions of the wing were calculated as:

$$b = 4.66\ ft$$

$$c = 0.777\ ft$$

2.5 Tail sizing

The distance between the aerodynamic center of the wing and the horizontal tail was chosen as 1.5 ft as a starting point. From there, the recommended initial tail volume coefficient of 0.5, and with the chord determined, the horizontal tail area was calculated using Equation 10.

$$S_H = 0.937\ ft^2$$

An initial AR for the horizontal tail of 3 was chosen to ensure that the tail had enough structural stability. As a result, the dimensions for the horizontal tail were:

$$b_H = 1.68\ ft$$

$$c_H = 0.559\ ft$$

These numbers were then used to conduct a stability analysis for the aircraft. From there, iterations can be made to achieve the desired stability. For future years, when the aircraft is further in the design stage, weight simulation can be added to the model in XFLR5, which will help the model yield more accurate results for the stability analysis. As a result, it is recommended that the dimensions for the tail be optimized after a more concrete weight and moment of inertia of the aircraft are determined.

The distance between the aerodynamic center of the wing and the horizontal tail was assumed to be the same as the horizontal tail. From there, with an AR of 1.2, the dimensions for the vertical tail were:

$$b_V = 0.735\ ft$$

$$c_V = 0.612\ ft$$

2.6 Control surface sizing

For the NACA 2415 airfoil, the change in zero-lift angle of attack was calculated based on Equation 12 with 20% flap and the flap angle of 15°. The result was compared to the XFLR5 simulation of the airfoil with flap configuration. The results are shown in Table 6.

Table 6: Change in zero-lift angle of attack comparison

Method	Empirical (Equation 10)	XFLR5 simulation
$\Delta\alpha_0$	$-3.45°$	$-3.25°$

As seen in Table 6, Sadraey's empirical method to calculate the change in zero-lift angle of attack for the airfoil was significantly close to the XFLR5 simulation results, with an error of only 6%. Therefore, the relationship in Equation 10 can be used for quick initial calculations for the change of flap configuration; this was employed within the MATLAB code to calculate the lift coefficient of the wing with flap down configuration.

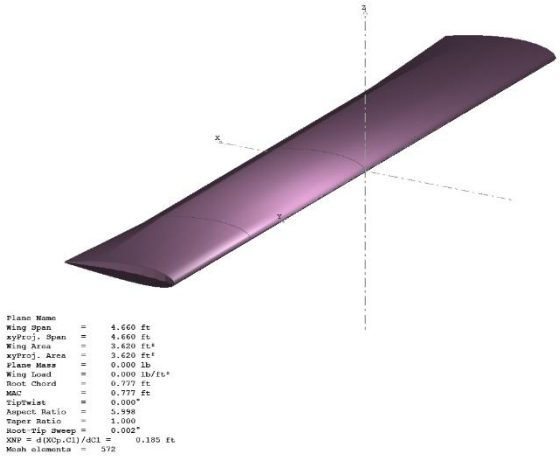

Figure 8: XFLR5 simulation of wing with flaps

The total span of the flaps was chosen to be 60% of the whole span of the wing as an initial design point. The code was tested with the wing at an angle of attack of 8°, and XFLR5 was again used to compare the lift coefficient (Figure 8). The results are shown in Table 7:

Table 7: Lift coefficient comparison

Method	Lifting-line (MATLAB)	XFLR5 simulation
C_{L_TO}	1.03	1.27

As seen in Table 7, the lifting-line underpredicted lift of the wing by around 19%. As a result, the lifting-line theory showed a more conservative way to design the control surfaces of the wing. However, more sophisticated simulations, such as XFLR5, can be used to allow for more design options.

With a stall speed of 35 ft/s, the required lift coefficient was calculated as:

$$C_{L\_TO\_req} = 0.993$$

Therefore, with a flap span of 60% total wingspan and flap chord of 20% total wing chord, the lift coefficient required was satisfied, through both the lifting-line theory and the XFLR5 simulation. In the future, CFD can also be used to compare with these methods, and it can also be used as a useful tool for validation. With a power estimation of 467 ft/lb.s based on propulsion calculations, the takeoff length was simulated using MATLAB as shown in Figure 9.

2.7 Takeoff distance

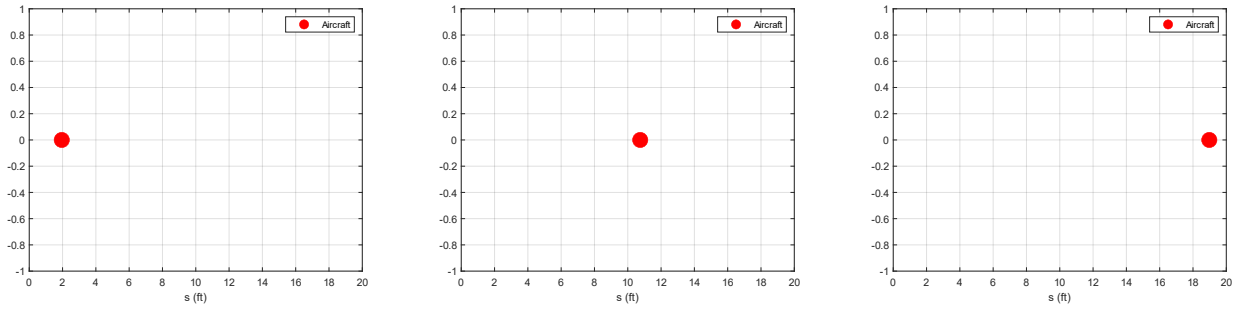

Figure 9: Takeoff simulation for the aircraft

The total takeoff distance estimated was estimated to be 19.2 ft which was within the 25 ft requirement. With the MATLAB script, the takeoff distance can be estimated for different power inputs, different wing sizing, and aerodynamic coefficients. As a result, it can be used as a tool to assist in the sizing and control surface determination for the aircraft.

The takeoff estimation assumes that the power of the motor is constant, and thrust is invertedly proportional to the power through velocity. In the future, different thrust estimation functions can also be used to model the relationship between thrust and power of the aircraft to obtain more accurate results. However, these methods only show an estimation of the takeoff distance, and flight testing must be conducted in order to confirm the results or iterate on the design.

IV. Conclusion

In conclusion, different methods were explored for the conceptual and preliminary design phase for aircraft. For the conceptual design phase, trade studies were conducted through decision matrices and logical evaluations. From there, elements (such as wing location, wing planform, and tail configuration) were selected for an initial design for the aircraft. For the preliminary design phase, other parameters (such as weight, wing dimensions, tail dimensions, etc.) were determined through calculations conducted using analytical tools and numerical simulations. However, the dimensions obtained were only a starting point and require refinement through the later stages of the design process. By and large, the project successfully introduced a road map for the conceptual and preliminary design phase, and it can be used as a foundation for a design of a DBF aircraft.

Appendix A: MATLAB Code

DesignRegion.m

```
close all
clear all

%% Givens
W = 7.24; % Weight [lb]
Vstall = 35; % Stall Speed [ft/s]
Vmax = 98.4; % Max speed [ft/s]
AR = 6; % Aspect ratio
Cd0 = 0.0325; % Assumed parasite drag coeff
Sto = 25; % Take off distance [ft]
rho = 0.002274; % Density [slugs/ft^3]
CLmax = 1.5; % Sadraey recommended initial max Cl
eta = 0.75; % Assumed efficiency
e = 0.78; % Assumed Oswald coeff

% Assumed parameters based on Sadraey recommendations
f_coeff = 0.04;
CdLG = 0.009;
Cdhld = 0.005;
Clc = 0.3;
Cl_flap = 0.3;
ROC = 10; % Rate of climb [ft/s]
L_Dmax = 9;
rhos = 0.00238;

%% Calculate terms used for the functions
Vto = 1.25*Vstall;
Cd0to = Cd0 + CdLG + Cdhld;
Clto = Clc + Cl_flap;
K = 1/pi/AR/e;
CdTO = Cd0to + K*Clto^2;
CdG = CdTO - f_coeff*Clto;
ClR = CLmax/1.1^2;
sigma = rho/rhos;

%% Calculate the correponding functions of W/P vs W/S
% Function of stall speed
WS = 1/2*rhos*Vstall^2*CLmax;
x = linspace(0.1,19.1,100);
x0 = WS*ones(1,length(x));
y0 = linspace(0,350,length(x));

% Function of max speed
WPvmax = eta./(0.5*rhos*Vmax^3*Cd0./x + 2*K.*x/rho/sigma/Vmax)*550;

% Function of takeoff distance
x1 = exp(0.6*rho*32.2*Sto*CdG*1./x);
WPTO = (1-x1)./(f_coeff-(f_coeff+CdG/ClR).*x1)*eta/Vto*550;

% Fucntion of rate of climb
WPROC = 1./(ROC/eta+sqrt(2/rho/sqrt(3*Cd0/K).*x)*1.155/L_Dmax/eta)*550;

% Function of max altitude
WPAC = sigma./(sqrt(2/rho/sqrt(3*Cd0/K).*x)*1.155/L_Dmax/eta)*550;

%% Design point (Plotting purpose only)
xdp = 1.95;
ydp = 5.5;

%% Plot the results
figure
hold on
plot(x0,y0,'linewidth',1.25,'color','b')
```

```
plot(x,WPvmax,'linewidth',1.25,'color','r')
plot(x,WPTO,'linewidth',1.25)
plot(x,WPROC,'linewidth',1.25,'color','m')
plot(x,WPAC,'linewidth',1.25)
plot(xdp,ydp,'or','MarkerFaceColor','r','MarkerSize',5,'MarkerEdgeColor','k')
xlim([0 18])
ylim([0,100])
legend('V_{stall}','V_{max}','L_{TO}','Rate Of Climb','Max Altitude','Design Point')
grid on
```

WingDesignNACA2415.m

```
clc
close all
clear all

%% Givens
W = 7.24; % Estimated weight [lb]
Vs = 35; % Stall speed [ft/s]
Vc = 82; % Cruise speed [ft/s]
Vto = 1.2*Vs; % Take off speed [ft/s]
Vmax = 1.2*Vc; % Max speed [ft/s]
W_S = 2; % Wing loading [lb/ft^2]
S = W/W_S; % Planform area

rho = 0.002274; % Flight density [slugs/ft^3]
rho0 = 0.002283; % Take off desity [slugs/ft^3]

del_to = 15; % Take off flap config
del_l = 30; % Max flap config

%% Calculate sectio lift coefficient for airfoil
C_Lc = W/(0.5*rho*Vc^2*S);
C_Lcw = C_Lc/0.95;
C_l = C_Lcw/0.9; % Ideal cruise lift coeff for airfoil

C_Lmax = W/(0.5*rho0*Vs^2*S);
C_Lmaxw = C_Lmax/0.95;
C_lmax_gross = C_Lmaxw/0.9; % Max cruise lift coeff for airfoil
% C_lmax = C_lmax_gross - 0.9*(del_to/60);
C_lmax = C_lmax_gross/1.25; % Plain flap assumption

%% Required take off lift coefficient
C_L_to_req = W/(0.5*rho0*Vto^2*S);

%% Lifting-line Theory [Sadraey]
N = 26; % (number of segments-1)
AR = 6; % Aspect ratio
lambda = 1; % Taper ratio
i_w = 8; % wing setting angle (deg)

cf_c = 0.2;
bf_b = 0.6; % flap-to-wing span ratio
del_alpha = -1.15*cf_c*del_to;

a_2d = 6.108; % lift curve slope (1/rad)
a_0 = -2.25; % flap up zero-lift angle of attack (deg)
a_0_fd = a_0 + del_alpha; % flap down zero-lift angle of attack (deg)

b = sqrt(AR*S); % wing span
MAC = S/b; % Mean Aerodynamic Chord
Croot = (1.5*(1+lambda)*MAC)/(1+lambda+lambda^2); % root chord
theta = pi/(2*N):pi/(2*N):pi/2;
alpha = i_w*ones(1,N);

% segment's angle of attack
```

```
for i=1:N
    if (i/N)>(1-bf_b)
        alpha_0(i)=a_0_fd; %flap down zero lift AOA
    else
        alpha_0(i)=a_0; %flap up zero lift AOA
    end
end

z = (b/2)*cos(theta);
c = Croot * (1 - (1-lambda)*cos(theta)); % MAC at each segment
mu = c * a_2d / (4 * b);

LHS = mu .* (alpha-alpha_0)/57.3; % Left Hand Side
% Solving N equations to find coefficients A(i):
for i=1:N
    for j=1:N
        B(i,j) = sin((2*j-1) * theta(i)) * (1 + (mu(i) *...
                (2*j-1)) / sin(theta(i)));
    end
end
A=B\transpose(LHS);

for i = 1:N
    sum1(i) = 0;
    sum2(i) = 0;
    for j = 1 : N
        sum1(i) = sum1(i) + (2*j-1) * A(j)...
                  *sin((2*j-1)*theta(i));
        sum2(i) = sum2(i) + A(j)*sin((2*j-1)*theta(i));
    end
end

%% Compare the lift coefficient required to the lift coefficent produced
CL_TO = pi * AR * A(1)
CL_TO - C_L_to_req
```

TailDesignNACA0009.m

```
clc
close all
clear all

%% Given
W = 7.24; % Estimated weight [lb]
Vs = 35; % Stall speed [ft/s]
Vc = 82; % Cruise speed [ft/s]
Vto = 1.2*Vs; % Take off speed [ft/s]
Vmax = 1.2*Vc; % Max speed [ft/s]
W_S = 2; % Wing loading [lb/ft^2]
S = W/W_S; % Planform area

rho = 0.002274; % Flight density [slugs/ft^3]
rho0 = 0.002283; % Take off desity [slugs/ft^3]

%% NACA 2415
Cmo = -0.02; % Wing airfoil moment coeffcient
AR = 6; % Wing AR
sweep = 0;
twist = 0;
alpha_s = 16.25; % Stall angle [deg]
i_w = 0.75; % Wing incident angle [deg]
a0_w = 6.108; % Lift curve slope [1/rad]

b = sqrt(AR*S);
c = S/b;
```

```
%% Horizontal Tail NACA 0009
ho = 0.25; % Normalized (wrt c) distance of ac from wing leading edge
h = 0.2; % Normalized (wrt c) distance of cg from wing leading edge
eta_h = 0.9; % Wing efficiency
V_h = 0.5; % Tail volume coefficient
K_c = 1.3; % Optimum tail arm correction factor
Df = 3.83; % Fuslage aft diameter
AR_h = 3; % Horizontal tail AR
a0_h = 6.7; % Section lift curve slope
e = 0.9; % Assumed Oswald efficiency

%% Vertical Tail NACA 0009
V_v = 0.04; % Vertical Tail volume coefficient
a0_v = 6.7; % Section lift curve slope
AR_v = 1.2; % Vertical Tail AR

%% Horizontal Tail Design
CL = W/(0.5*rho*Vc^2*S);

% Estimation for wing-fuslage moment coeff - Sadraey
Cm_wf = Cmo*(AR*cos(sweep)^2)/(AR+2*cos(sweep)) + 0.01*twist;

CL_h = (Cm_wf + CL*(h-ho))/eta_h/V_h; % Tail lift coefficient

l = 1.5; % Assumed tail arm

S_h = V_h*c*S/l; % Tail planform area

a_h = a0_h/(1+a0_h/pi/AR_h/e); % 3D Wing lift curve slope [1/rad]

a_h_deg = a_h/57.3; % [1/deg]

i_h = CL_h/a_h_deg; % Incident Angle

b_h = sqrt(S_h*AR_h); % Horizontal tail span
c_h = S_h/b_h; % Horizontal tail chord

h_t = l*tand(alpha_s - i_w - 3); % Vertical position of tail

a_w = a0_w/(1+a0_w/pi/AR/e); % Wing lift curve slope

deda = 2*a_w/pi/AR; % Change of downwash angle wrt to alpha

% Static longitudinal stability
Cm_alpha = a_w*(h-ho) - a_h*eta_h*S_h/S*(l/c-h)*(1-deda);

%% Vertical tail
% Assume the vertical tail has the same tail arm
l_v = l;

S_v = V_v*b*S/l_v; % Vertical tail area

b_v = sqrt(S_v*AR_v); % Vertical tail span
c_v = S_v/b_v; % Vertical tail chord
```

TakeOff.m

```
close all
clear all

%% Givens
P = 467.61; % [ft/lb.s] Max power
rho = 0.00238; % [slug/ft^3] Air density
W = 7.24; % [lb] Weight
m = W/32.2; % [slugs]
```

```
mu = 0.4; % Kinetic friction coefficient
S = 3.62; % [ft^2]
AR = 6; % Aspect ration
e = 0.78; % Assumed Oswald coeff

Cd0 = 0.0075; % Parasite drag
CL = 0.73; % Lift coefficient with flaps at 0 deg
Vto = 42; % Take off velocity

%% Velocity
dt = 0.0001; % Time step
v = 0.5; % Initial velocity
v_store = [];

% Initialize variables
L = 0; % Lift [lb]
x = 0; % Distance [ft]
y = 0;
i = 0; % Counter

while (W - L) > 0.1
    %% Store velocity and integrate to get distance
    v_store = [v_store; v];
    x = x + v*dt;
    i = i + 1;
    %% Plot results
    if mod(i,100) == 0
        plot(x,y,'ro','MarkerSize',15,'MarkerFaceColor','r')
        grid on
        legend('Aircraft')
        xlabel('s (ft)')
        xlim([0 20])
        ylim([-1 1])
        pause(0.01)
    end
    %% Calculate drag and lift
    D = 1/2*rho*v^2*(Cd0 + CL^2/pi/AR/e)*S;
    L = 1/2*rho*v^2*CL*S;
    %% March forward in time
    v = v + dt/m*(P/v - D - mu*(W-L));
end

%% Take off distance
fprintf('The take off distance is %.3f ft\n',x)
```

Appendix B: Components weight for UML DBF 2021

Table B1: Components weight for UML DBF aircraft 2021

Component	**Quantity**	**Weight (oz)**	**Total weight (oz)**
Motor	1	12.2	12.2
Battery	1	14.1	14.1
Speed Controller	1	5.10	5.10
Propeller	1	1.30	1.30
Servo	4	0.420	1.68
Total			34.4

Since the majority of the empty weight are the components, the total component weights can be used as an initial estimation for the empty weight.

$$W_E = 34.4\ oz = 2.15\ lb$$

Reference

[1] Sadraey, M. H., *Aircraft Design: A Systems Engineering Approach*, 1st ed., Wiley, Chichester, West Sussex, U.K., 2013.

[2] *Winning Reports 2012*, https://www.aiaa.org/docs/default-source/uploadedfiles/aiaadbf/previous-competitions/top-reports/2012-dbf-top-reports14d477c73ce34fb989035ff9d84c6fef.pdf?sfvrsn=19232ed1_0

[3] *Winning Reports 2008*, https://www.aiaa.org/docs/default-source/uploadedfiles/aiaadbf/previous-competitions/top-reports/2008-dbf-top-reports5d16838a3c3a4b4f85ba72c6a0a1b99a.pdf?sfvrsn=94eb64a9_0

[4] *Winning Reports 2017*, https://www.aiaa.org/docs/default-source/uploadedfiles/aiaadbf/previous-competitions/top-reports/2017topreports.pdf?sfvrsn=4aecc31f_2

[5] *Winning Reports 2016*, https://www.aiaa.org/docs/default-source/uploadedfiles/aiaadbf/previous-competitions/top-reports/2016-dbf-top-reports35c1e6260e28477681353b8c4c4a195b.pdf?sfvrsn=4cc4cf58_0